

Hot Spot Stress Determination for a Tubular T-Joint under Combined Axial and Bending Loading

M. Haghpanahi and H. Pirali

Abstract: Finite element analysis of a tubular T-joint subjected to various loading conditions including pure axial loading, pure in-plane bending (IPB) and different ratios of axial loading to in-plane bending loading has been carried out. This effort has been established to estimate magnitudes of the peak hot spot stresses (HSS) at the brace/chord intersection and to find the corresponding locations as well, since, in reality, offshore tubular structures are subjected to combined loading, and hence fatigue life of these structures is affected by combined loading. Therefore in this paper, at the first step, stress concentration factors (SCFs) for pure axial loading and in-plane bending loading are calculated using different parametric equations and finite element method (FEM). At the next step, the peak HSS distributions around the brace/chord intersection are presented and verified by the results obtained from the API RP2A Code procedure. Also the locations of the peak hot spot stresses which are the critical points in fatigue life assessment have been predicted.

Keywords: Finite Element Method, Hot Spot Stress, Tubular Joint, Stress Concentration Factor, Parametric Equations

1. Introduction

The Hot Spot Stress (HSS) approach is typically used for fatigue-resistant design and/or the durability approval of welded offshore tubular joints [1]. Traditional approach of fatigue life prediction for the offshore tubular joints employs a HSS range versus number of cycles (S-N) curve based on large-scale fatigue tests on tubular joints [2].

Therefore it is very important to use an appropriate method for estimation of HSS in tubular joints as well as determination of corresponding locations. There are several methods available for estimating the hot spot stresses. Each method has its own advantages and disadvantages.

The experimental method, is a well-known method for estimating the HSS at the brace/chord intersection. But this method is time-consuming and costly. Another method for HSS determination, commonly used in tubular joints, is the calculation of stress concentration factors using available parametric equations followed by usage of some specific codes such as API RP2A code and Department of Energy Guidance Notes reported for estimation of peak HSS under combined loading [3,4].

Here it should be noted that these parametric equations are valid only for a limited range of non-dimensional geometric parameters. Also it should be mentioned that these equations usually are not able to specify the location of the critical points and they don't consider the weld geometry.

There are several parametric equations proposed for estimation of stress concentration factors in tubular joints. The Kuang equations [5] (1975) cover T/Y, K and KT joints configurations and utilize a modified thin-shell finite element program specifically designed to analyze tubular connections.

The tubular connections were modeled without a weld fillet. The Wordsworth/Smedley (1978) equations were derived using acrylic model test results on tubular joints modeled without a weld fillet [6].

The UEG equations proposed in 1985 [4] are based on the W/S and Wordsworth equations with a modification factor applied to configurations with high β ($\beta > 0.6$) or high γ ($\gamma > 20$) values.

In 1985 Efthymiou and Durkin [7] published a series of parametric equations covering T/Y and gap overlap K joints. Over 150 configurations were analyzed via the PMBSHELL finite element program using 3-dimensional shell elements and the results were checked against the SATE finite element program for one T-joint and 2 K-joint configurations.

Received by the editor October, 11, 2004; final revised: April, 22, 2006.

M. Haghpanahi is an Associate Professor of Mechanical Engineering, Iran University of Science and Technology, mhaghpanahi@yahoo.com

H. Pirali is a Ph.D Student at the Department. hpirali@iust.ac.ir

The Hellier, Connolly and Dover (HCD) equations [8] were published in 1990.

These equations primarily developed to improve fracture mechanics estimates of remaining life for a joint rather than designing a tubular joint.

Consequently the overall program included not only HSS estimates, but also modeling of the stress distribution around the brace chord intersection and the proportions of bending to axial stress through the member thickness. The Lloyd's Register (LR) equations [9] were developed as a part of the "SCFs for simple tubular joints" project which was largely funded by the "Health and Safety Executive" (HSE), in 1991. Parametric equations mentioned above are mainly based on the finite element analysis using shell elements. Therefore, if in the finite element analysis of tubular joints, shell elements are employed, more consistent results will be obtained comparing to the usage of solid elements. Owing to limitations and difficulties for HSS estimation of tubular joints and complex geometrical nature of most tubular joints, finite element method may be considered as one of the most efficient numerical methods for performing stress analysis on tubular joints. The major concern of this paper is calculation of stress concentration factors in pure axial loading and in-plane bending followed by the estimation of peak HSS magnitudes and locations at the brace/chord intersection under combined axial loading plus in-plane bending.

2. Joint Classification of Tubular Joints

For the purpose of SCF evaluation, tubular joints are usually classified into joint types T/Y, X, K or KT joints. Each joint type has its own geometric parameters. These parameters for a T/Y joint are shown in Fig (1). The geometric parameters needed to define each joint type, e.g. chord diameter (D), chord thickness (T), brace diameter (d), brace thickness (t), etc. are defined in the figure. Appropriate non-dimensional geometric parameters b, g, t, a, q are also defined in the Fig(1). The parametric equations for estimation of SCFs are based on non-dimensional geometric parameters rather than the original geometric parameters such as D, T, L, d, t. This way of definition simplifies the equations and makes it easy to simulate large models with small models having the same non-dimensional geometric parameters. The T-joint investigated in this paper as shown in Fig (2) has a chord diameter of D=500 mm, chord thickness T=16 mm, chord length L=4000 mm, brace diameter d=400 mm, brace thickness t=10 mm and non-dimensional parameters as follows:

$$\beta = 0.8, \gamma = 15.625, \tau = 0.625, \alpha = 16, \theta = 90$$

3. Calculation of Stress Concentration Factors

The stress concentration factor of a tubular joint subjected to a particular loading is defined as the ratio of the absolute maximum principal stress (i.e. HSS),

which occurs at the brace/chord intersection, to the nominal stress of the brace [10].

Generally, stress concentration factors (SCFs) may be derived from finite element analysis (FEA); model tests or empirical equations based on such methods. Each method has its own advantages and disadvantages. The finite element method is ideally suited for estimation of SCFs in complex geometries.

When deriving SCFs using FE analysis it is possible to use shell elements, volume (solid) elements to present the weld region (as opposed to thin shell elements) or combined shell and solid elements.

Considering Fig(3), The SCFs can be derived by extrapolating stress components to the relevant weld toes and combining these to obtain the maximum principal stress and hence the SCF. Note that as shown in Fig (3), the stress distribution changes rapidly near the weld toe and extrapolation distances must be the same as the distances shown in Fig (3) to prevent significant errors during determination of SCFs.

The extrapolation direction should be normal to the weld toes as shown in Fig(3). If thin shell elements are used, the results should be interpreted carefully since no single method is guaranteed to provide consistently accurate stresses. The extrapolation shall be based on the surface stress, i.e. not the midline stress for shell models. The surface stress is to be based on average nodal stress [11].

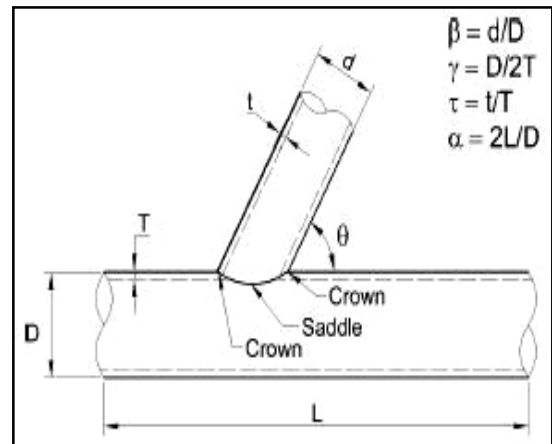


Fig. 1. Geometric Parameters for a T or Y Joint

When deriving SCFs from model tests, care should be taken to cover all potential hot spot locations with strain gauges. Further, it should be recognized that the strain concentration factor is not identical to the SCF but is related to it via the transverse strains and poisson's ratio. If the chord length in the joint tested is less than about 6 diameters ($a < 12$), the SCFs may need to be corrected using the Efthymiou short chord correction factors. The same correction may be needed in FE analysis if $a < 12$ [12].

In this paper, finite element method and some parametric equations are used for estimation of SCFs under axial and IPB loading.

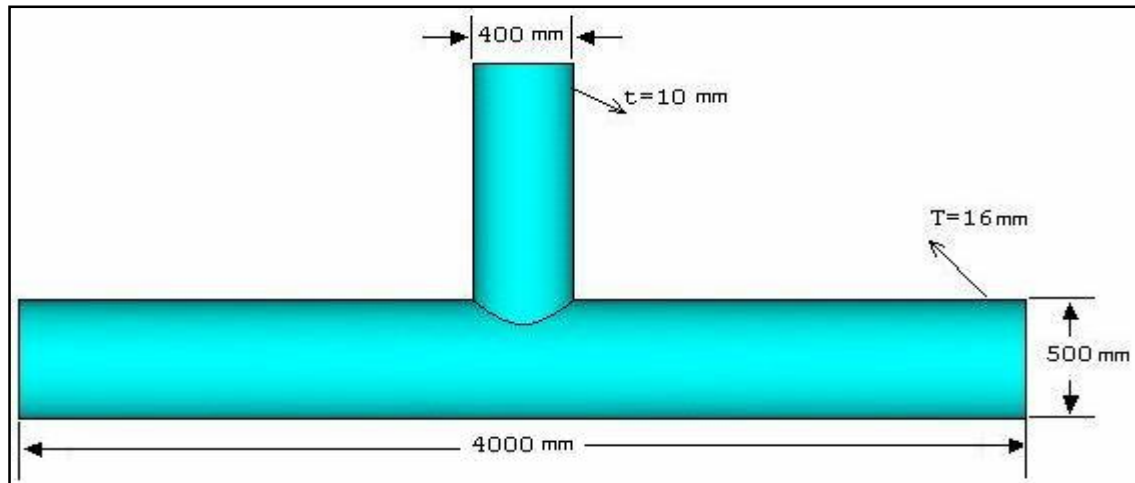


Fig. 2. Geometrical Parameters of The Investigated Joint

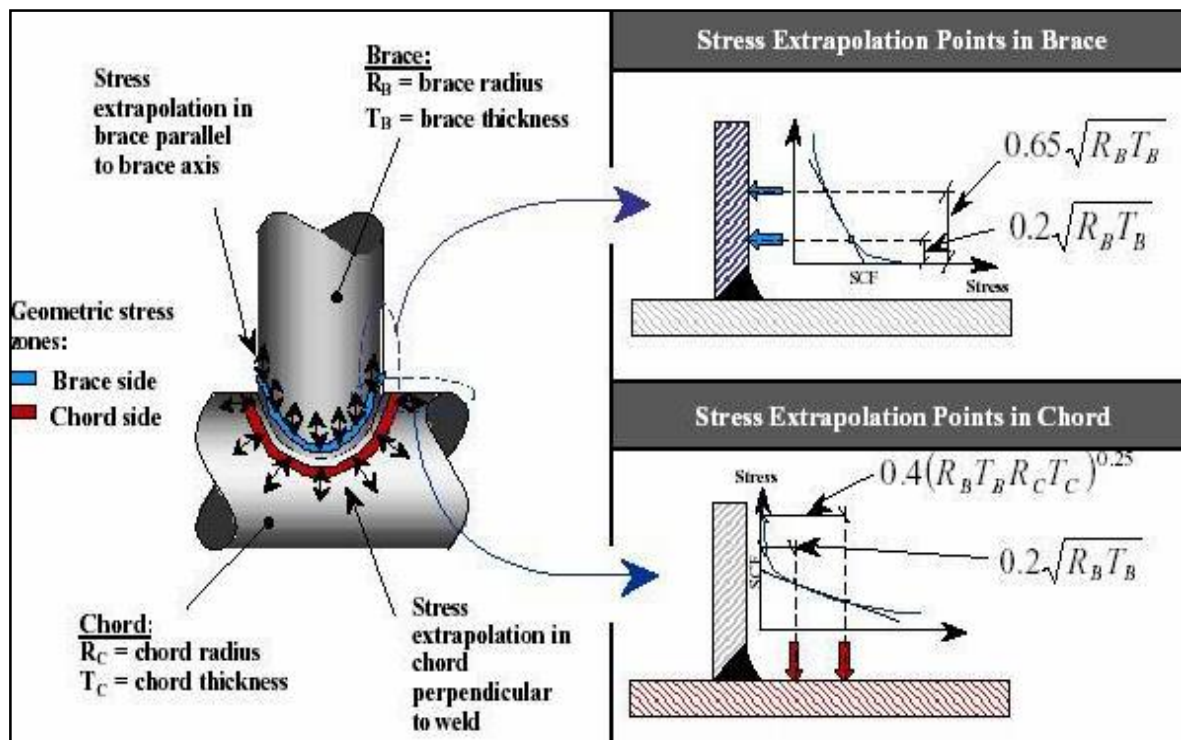


Fig. 3. Stress Extrapolation Procedure for Determination of S.C.F

4. Calculation of SCFs Using Parametric Equations

The parametric equations proposed by LR for estimation of SCFs for tubular T-joints are presented in Fig (4). The results of SCF calculation for the selected T-joint in axial and IPB loading conditions are listed in Table (1).

Referring to this table, it can be seen that by using some sets of the proposed methods such as EFTHYMIUO and LR, the SCF results can be predicted exactly at the saddle or crown position.

Also it is clear that there is a good agreement of SCF results using different methods.

In this study the LR method, which is the most recent among all of the mentioned methods, is considered as a benchmark reference to verify the finite element results.

5. Calculation of SCFs Using FEM

For the finite element analysis of the selected T-joint, commercial FEM code ANSYS is used. Finite element model of the joint is shown in Fig (5). The element used for the analyses is shell 93 which is a second order shell element. Because of symmetry, only a half of the T-joint is modeled to reduce the number of elements and hence the run time. Symmetry boundary conditions are applied to the plane of symmetry and the ends of the chord are modeled as fully fixed. The applied load is in the form of pressure exerted at the top of the brace. In the finite element analysis, a local mesh refinement at the brace/chord intersection which has highly nonlinear stress distribution behavior, is constructed to get more accurate results at this region. For clarity an enlarged view of the finite element model is illustrated in Fig (5).

It should be noted that the finite element results are derived for chord side. Figures (6) and (7) show the results of SCF calculations in axial and IPB loading by extrapolating the maximum principal stresses normal to the weld toe as supposed earlier. Referring to Fig (3), distances for linear extrapolation must lie within the $0.2\sqrt{R_b T_b}$ to $0.4\sqrt{R_b T_b R_c T_c}$, in this case 8.94 mm to 21.27 mm. From the previous results reported in Table (1), and comparing them to the finite element results, it can be seen that there is a good agreement between the results of FEM and parametric equations.

6. Hot Spot Stress Determination Using Parametric Equations and API RP2A CODE

As mentioned before, for estimation of the peak hot spot stresses, in the case of combined loading, some special

methods such as American Petroleum Institute API RP2A code may be employed. This method is used in offshore industry to estimate the peak HSS in combined loading using an elastic superposition procedure. The associated equation is as follows[2]:

Peak HSS=

$$SCF_{AX} F_{AX} + \sqrt{(SCF_{IPB} F_{IPB})^2 + (SCF_{OPB} F_{OPB})^2}$$

Where $SCF_{AX}, SCF_{IPB}, SCF_{OPB}$ are stress concentration factors in axial, in-plane bending and out-of-plane bending respectively and F_{AX}, F_{IPB}, F_{OPB} are the nominal brace stresses in axial, in-plane bending and out-of-plane bending respectively. The obtained results using this method are given in Table (2).

Axial	IPB						
Chord Saddle: $\tau\gamma^{1.2}(2.12 - 2\beta) \sin^2\theta$	Chord: $1.22\tau^{0.8}\beta\gamma^{(1-0.68\beta)} \sin^{(1-\beta^3)}\theta$						
Chord Crown: $\tau\gamma^{0.2}(3.5 - 2.4\beta) \sin^{0.3}\theta + B0.B1$	Brace: $1 + \beta\tau^{0.2}\gamma(0.26 - 0.21\beta) \sin^{1.5}\theta$						
Brace Saddle: $1 + \tau^{0.6}\gamma^{1.3}\beta(0.76 - 0.7\beta) \sin^{2.2}\theta$							
Brace Crown: $2.6\beta^{0.65}\gamma^{(0.3-0.5\beta)}$							
$B0 = \frac{0.7\tau(\beta - \tau/2\gamma)(\alpha/2 - \beta/\sin\theta) \sin\theta}{(1 - 3/2\gamma)}$							
$B1 = 1.05 + \frac{30\tau^{1.5}(1.2 - \beta)(\cos^4\theta + 0.15)}{\gamma}$							
	<table border="1"> <thead> <tr> <th style="text-align: center;">Validity Range</th> </tr> </thead> <tbody> <tr> <td style="text-align: center;">$0.13 \leq \beta \leq 1.0$</td> </tr> <tr> <td style="text-align: center;">$0.25 \leq \tau \leq 1.0$</td> </tr> <tr> <td style="text-align: center;">$10 \leq \gamma \leq 35$</td> </tr> <tr> <td style="text-align: center;">$30^\circ \leq \theta \leq 90^\circ$</td> </tr> <tr> <td style="text-align: center;">$\alpha \geq 4$</td> </tr> </tbody> </table>	Validity Range	$0.13 \leq \beta \leq 1.0$	$0.25 \leq \tau \leq 1.0$	$10 \leq \gamma \leq 35$	$30^\circ \leq \theta \leq 90^\circ$	$\alpha \geq 4$
Validity Range							
$0.13 \leq \beta \leq 1.0$							
$0.25 \leq \tau \leq 1.0$							
$10 \leq \gamma \leq 35$							
$30^\circ \leq \theta \leq 90^\circ$							
$\alpha \geq 4$							

Fig. 4. SCFs Proposed by LR for Tubular T-Joints

7. Hot Spot Stress Distribution Around the Brace/Chord Intersection Supported by FEM

Figures 8 to 11 show the distribution of the hot spot stresses around the brace/chord intersection under axial, IPB, combined loading at fixed axial loading and combined loading at fixed IPB loading respectively. In each figure, the peak locations on the curves indicate to the peak hot spot stresses. These critical points are circled in the figures. Fig (8) shows the HSS distribution at the brace/chord intersection under pure axial loading.

As a general rule, for these types of tubular joints, the critical point is always located at the saddle point [2]. This note is confirmed in fig (8). Fig (9) shows the HSS distribution at the brace/chord intersection under pure axial loading. The critical point for these joints under IPB loading is located somewhere different from saddle or crown, approximately midway between the saddle and the crown. But the

exact location of the critical point depends on non-dimensional geometric parameters b, g [12].

In this case the peak HSS occurs approximately at 50° from the crown. In the case of combined loading, the peak HSS location varies between the crown and the saddle, depending on the ratio of axial to bending loading.

This fact is drawn in fig (10). But in fig (11), that the bending component of the combined load is set to a fixed value, this dependency is not significant and the critical point location is almost independent of the ratio of nominal axial to bending stress of the brace.

Finally a comparison between the peak HSS results obtained from API and those obtained from FEM are presented in Table (2) and it can be seen that the FEM results reasonably are in good agreement with API code procedure, especially in high ratios of axial to bending loading.

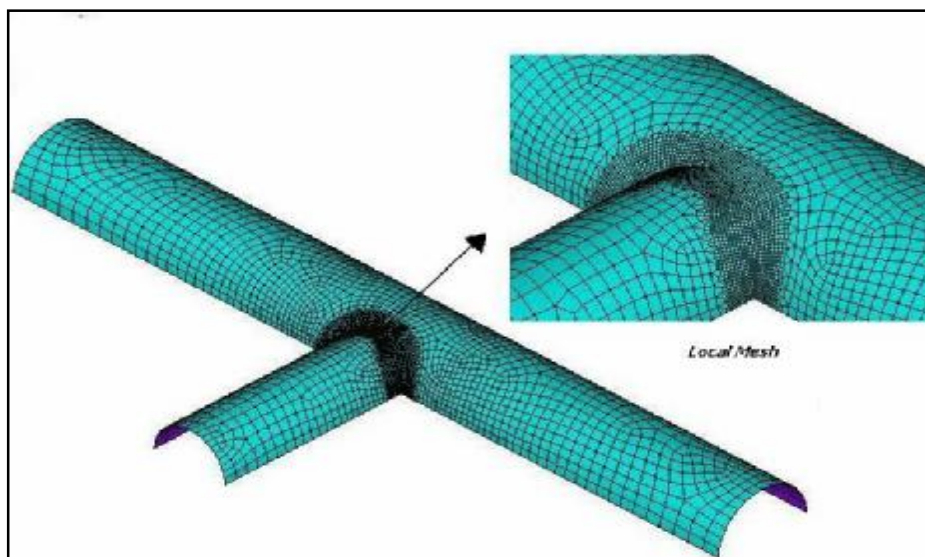


Fig. 5. Finite Element Model of Investigated T-Joint

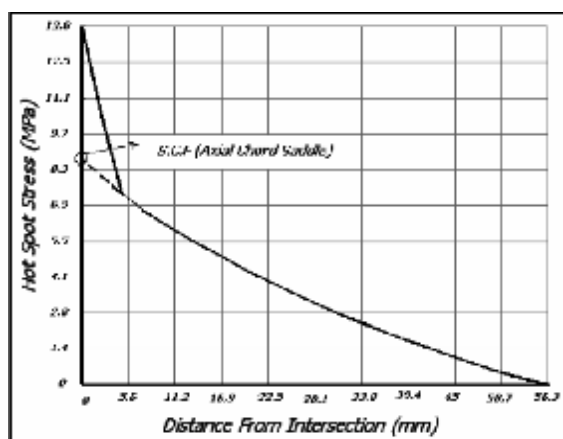


Fig. 6. Hot Spot Stress at The Brace/Chord Intersection

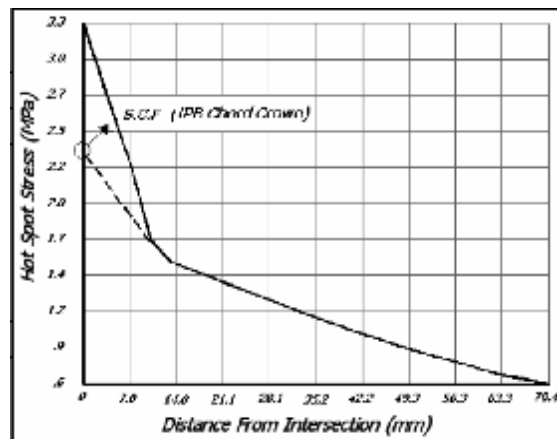


Fig.7. Hot Spot Stress at The Brace/Chord Intersection

Table 1. SCFs Calculated by Different Parametric Equations

EFTHYMIU	AXIAL				IPB	
	chord		brace		chord	brace
	saddle	crown	saddle	crown		
	8.05	3.49	6.83	2.3	2.72	2.58
KUANG	chord		brace		chord	brace
	8.06		6.42		2.45	2.22
GIBSTEIN	chord		brace		chord	brace
	7.3		7.89		2.44	2.11
LLOYDs REGISTER	chord		brace		chord	brace
	saddle	crown	saddle	crown		
	8.8	4.71	5.3	1.7	2.34	2.04

Table 2. A Comparison Between The Peak HSS Results Obtained From API and FEM

FAX	FIPB	RATIO	API	FEM	DIFF (%)
1	1	1	11.14	9.61	13.70
1	2	0.5	13.48	10.99	18.48
1	5	0.2	20.5	16.92	17.47
2	1	2	19.94	18.57	6.88
5	1	5	46.34	45.52	1.77

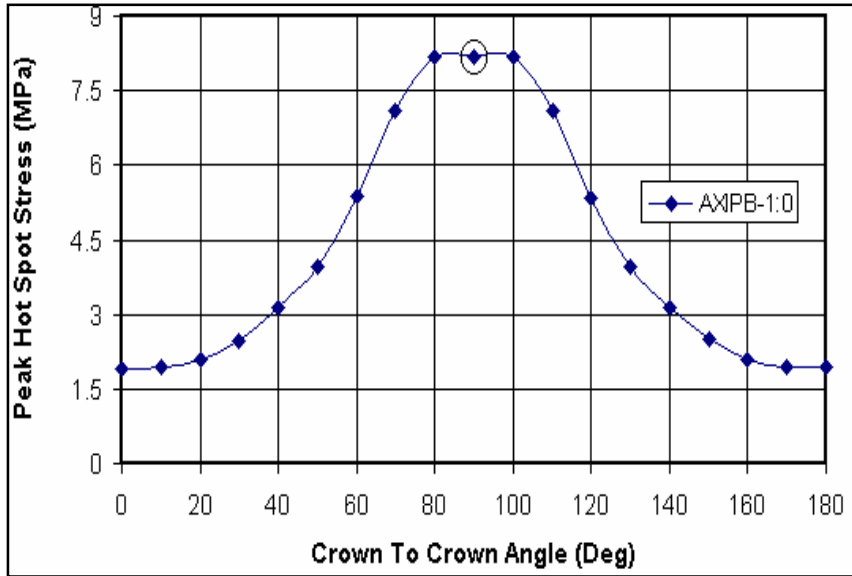


Fig. 8. Peak Hot Spot Stress Distribution Around The Brace/Chord Intersection

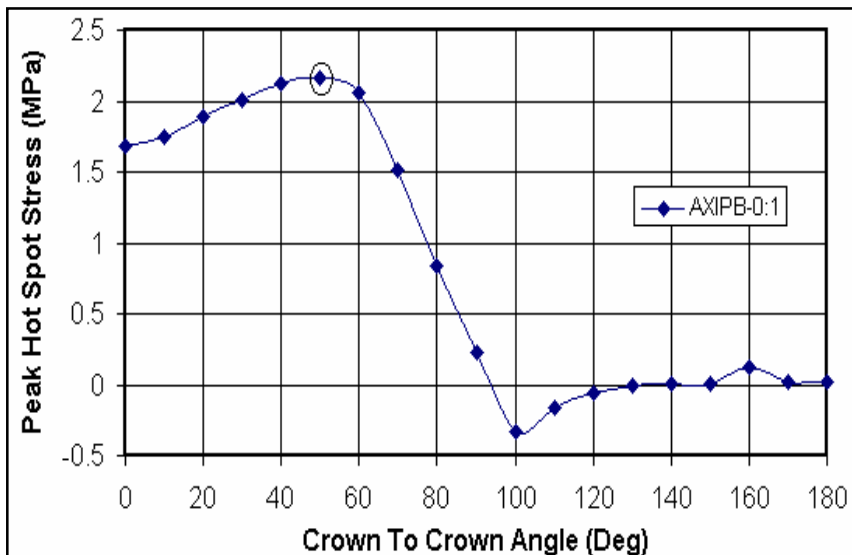


Fig. 9. Peak Hot Spot Stress Distribution Around The Brace/Chord Intersection

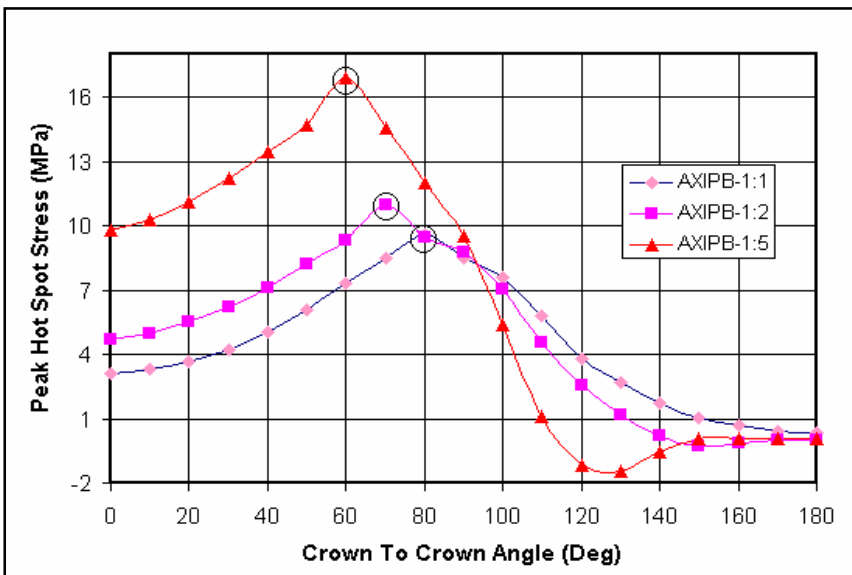


Fig. 10. Peak Hot Spot Stress Distribution Around The Brace/Chord Intersection

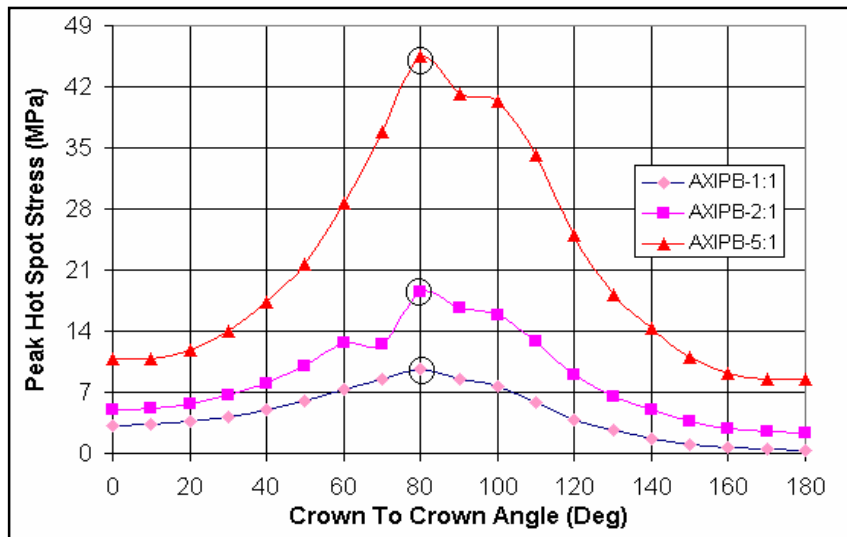


Fig. 11. Peak Hot Spot Stress Distribution Around The Brace/Chord Intersection

8. Conclusion and discussion

Hot spot stress determination for a tubular T-joint under combined axial and in-plane bending loading was carried out to investigate the peak hot spot stresses around the brace/chord intersection.

To do so, two methods were employed. The first method was based on the usage of different parametric equations expressed for estimation of stress concentration factors of tubular joints subjected to axial or in-plane bending loading, followed by API RP2A code which calculates the peak hot spot stresses under combined loading.

The second one was based on the usage of finite element method using shell elements. Obtained results showed that, if, in the finite element analysis, an appropriate stress extrapolation procedure is chosen, then there would be satisfactory agreement with parametric equations.

Similarly a good consistency of the finite element results will exist with API RP2A code, provided that the mentioned condition is satisfied.

In the finite element analysis, it was founded that in pure axial loading, the critical point is located on the saddle position while for the case of pure in-plane bending loading, this occurs almost midway between the saddle and the crown.

The finite element results of this study can provide valuable information for fatigue life assessment of offshore structures, since not only the peak hot spot stresses are known but also the locations of critical points around the brace/chord intersection which fatigue cracking is expected to occur, are estimated.

References

[1] Savaidis, G., Vormwald, M., "Hot-spot stress evaluation of fatigue in welded structural connections

supported by finite element analysis", Int.j.fatigue, vol. 22, pp. 85-91, 2000.

[2] Pang., H.L.J, Lee.C.W, "Three-dimensional finite element analysis of a tubular T-joint under combined axial and bending loading", Int.j.fatigue, vol. 17, no 5, pp313-320, 1995.

[3] "Recommended practice for planning. Designing and constructing fixed offshore platforms", API RP2A, 19th edn, American Petroleum Institute, Washington, DC, August 1991.

[4] "Background to new fatigue design guidance for steel welded joints in offshore structures", Report of the Department of Energy Guidance Notes, Revision Drafting Panel, HSMO, London, 1984.

[5] Kuang, J.G., Potvin, A.B. and Leick, R.D. In "Proc. 7th Annual Offshore Technology Conference", OTC 2205, Houston, TX, 1975, pp. 593-612.

[6] Wordsworth, A.C. and Smedley, G.P. In "Proc. European Offshore Steel Research Seminar", Cambridge, UK, November 1978, paper 31.

[7] Efthymiou, M. and Durkin, S. In "Proc. Conf. On Behavior of Offshore Structures", Delft, Elsevier Science Publishers, Amsterdam, 1985, pp. 429-440.

[8] Hellier, A.K., Connolly, M.P. and Dover, W.D. Int.J.Fatigue 1990. 12,13.

[9] Lloyd's Register of shipping, "Stress concentration factors for tubular complex joints", 1991.

[10] Pey. L.P, Soh. A.K, Soh. C.K, "Partial implementation of compatibility conditions in modeling tubular joints using brick and shell elements", finite

elements in analysis and design, vol. 20, pp. 127-138, 1995.

wind turbines and support structures", Det Norske Veritas (DNV), Denmark A/S, 2003.

[11] Jan, Behrendt Ibs f , "*Fatigue design of offshore*

[12] [http://www.galbraithconsulting.co.uk/iso/19902/iso/19902/ Clause _16_CD.PDF](http://www.galbraithconsulting.co.uk/iso/19902/iso/19902/Clause_16_CD.PDF)